PHYSICAL REVIEW A **83**, 053402 (2011)

Electron-positron pair creation induced by quantum-mechanical tunneling

M. Jiang,[1] W. Su,[2] X. Lu,[1] Z. M. Sheng,[1,3] Y. T. Li,[1] Y. J. Li,[2] J. Zhang,[1,3] R. Grobe,[4] and Q. Su[4,*]

[1]*Beijing National Laboratory for Condensed Matter Physics, Institute of Physics, Chinese Academy of Sciences, Beijing 100190, China*

[2]*China University of Mining and Technology, College of Sciences, Beijing 100083, China*

[3]*Key Laboratory for Laser Plasmas and Department of Physics, Shanghai Jiao Tong University, Shanghai 200240, China*

[4]*Intense Laser Physics Theory Unit and Department of Physics, Illinois State University, Normal, IL 61790-4560 USA*

(Received 21 January 2011; published 3 May 2011)

We study the creation of electron-positron pairs from the vacuum induced by two spatially displaced static electric fields. The strength and spatial width of each localized field is less than required for pair creation. If, however, the separation between the fields is less than the quantum-mechanical tunneling length associated with the corresponding quantum scattering system, the system produces a steady flux of electron-positron pairs. We compute the time dependence of the pair-creation probability by solving the Dirac equation numerically for various external field sequences. For the special case of two very narrow fields we provide an analytical expression for the pair-creation rate in the long-time limit.

DOI: 10.1103/PhysRevA.83.053402 PACS number(s): 34.50.Rk, 32.80.Wr, 12.20.Ds, 03.65.−w

I. INTRODUCTION

The creation of electron-positron pairs from the vacuum under an external supercritical electric force is one of the most fascinating subjects in quantum electrodynamics [1]. In 1951, Schwinger showed that a strong static electric field could break down the vacuum to generate a steady flux of electron-positron pairs [2]. Even though the theory does not require a precise threshold field strength, the typical field associated with such a pair creation is on the order of $\mathsf{E}_c = 1.32 \times 10^{16}$ V/cm. More recent theoretical investigations have shown that there is a second mechanism to create pairs. Even if the field strength is below E_c, pairs can be created if the external field varies rapidly in time, as is characteristic of a laser pulse [3–7].

So far all experimental attempts to observe this intriguing phenomenon of the direct conversion from light to particles in the lab have been unsuccessful. The pioneering experiment at SLAC [8] has observed a pair-production process triggered from collisions of an electron beam with an intense laser pulse. While this experiment was operated essentially in the perturbation domain, it did observe the onset of nonperturbative signatures [9,10]. Beginning in the 1980s attempts were made to create a supercritical field via two overlapping Coulomb fields associated with colliding heavy ions [11,12]. Positrons were measured but it is believed today that their main production mechanism was not necessarily caused by the Coulombic field itself, but triggered by nuclear transitions, which are unavoidable in highly relativistic collisions.

In order to reach the Schwinger limit in a more controllable environment with a time-varying external field, the laser intensity has to exceed $\sim 4 \times 10^{29}$ W/cm^2. The highest intensity level of high-power laser systems is presently $\sim 10^{22}$ W/cm^2, but there are tremendous efforts underway at various labs to approach the Schwinger limit and hopefully one day to observe a laser-only induced pair-creation process experimentally [13]. In view of the present difficulty to provide sufficiently strong fields, several theoretical proposals [14–17] to lower the threshold have been investigated involving combinations of static electric, magnetic, and time-dependent laser fields. In all cases the fields are required to overlap spatially and to be applied simultaneously.

In this work we show that there is a third and independent process that could also contribute to the creation of electron-positron pairs even if the external field is neither supercritical nor time dependent. This additional mechanism can be loosely associated with quantum-mechanical tunneling. It can be observed if two static and subcritical electric fields are separated by less than the quantum-mechanical tunneling length. It is worth mentioning that the pair creation initiated by quantum tunneling between spatially localized fields discussed here is fundamentally different from the constant field arrangement considered by Schwinger. For example, Schwinger's result does not require a threshold value for the field. However Schwinger's formula shows an exponential dependence on the electric field strength and is often associated with a tunneling-like process.

We compute the time dependence of the pair-creation probability and the positron spectra for such a two-field configuration from the quantum field operator. The operator's space and time dependence is obtained by solving the Dirac equation numerically [18–21]. This computational approach to quantum field theory has been introduced recently to study the pair-creation process with full space-time resolution. For a recent review, see Ref. [22]. It can provide an alternative approach to the traditional *S*-matrix approach, which is based on the in- and out-states only and therefore cannot visualize the processes inside the interaction zone. In addition to visualizing the details of the pair-creation dynamics, direct time-dependent quantum field theoretical solutions to the Dirac equation have also contributed to the resolution of various conceptual problems related to the negative energy states such as the Zitterbewegung [23], the relativistic localization problem [24], as well as the Klein paradox [25–28].

This paper is organized as follows. In Sec. II we introduce our model system characterized by two subcritical fields. In Sec. III we discuss how the quantum field theoretical pair-creation rate in the long-time limit can be related to the single-particle transmission coefficient of the corresponding quantum-mechanical system. In Sec. IV we compare our

*qcsu@ilstu.edu

numerical data with an analytical expression for the pair-creation rate that can be derived for the special case in which both fields are narrow. In Sec. V we provide a discussion of our results.

II. QUANTUM FIELD THEORETICAL SIMULATIONS

The interaction of electrons and positrons with external force fields is described by the Dirac equation (in atomic units),

$$i\partial\hat{\Psi}(t)/\partial t = [c\alpha_z p_z + \beta c^2 + V(z)]\hat{\Psi}(t), \qquad (1)$$

where $V(z)$ represents the scalar potential associated with the external force acting along the z direction. If we focus on that direction and only a single spin direction, the quantum field operator $\hat{\Psi}(z,t)$ has only two instead of the usual four components. In Eq. (1) α_z denotes the z component of the 2×2 Pauli matrix, β is the diagonal matrix, and c is the speed of light. As the details of how the time-dependent field operator and the associated fermionic operator algebra can be obtained numerically from Eq. (1) has been detailed in the literature [22], we present only a brief review in the Appendix. We also show there how the positive energy part of the field operator $\hat{\Psi}^{(p)}(z,t)$ can be used to compute the spatial density of the created electrons via the field theoretical expectation value in the initial vacuum state, $\rho(z,t) \equiv \langle\langle \text{vac}\|\hat{\Psi}^{\dagger(p)}(z,t)\hat{\Psi}^{(p)}(z,t)\|\text{vac}\rangle\rangle$. As the positive energy part of $\hat{\Psi}$ is based on free states, this density describes in a strict sense the true density only if the fields were instantaneously turned off [29,30]. This would include the possible changes in particle number due to the time dependence of the turnoff. The corresponding integral over all space, $N(t) = \int dz\rho(z,t)$, yields the time-dependent number of electron-positron pairs.

The specific configuration of external fields together with the associated potential is sketched in Fig. 1. The two electric fields have a width of W each and the maxima E_1 and E_2 are separated by a distance denoted by D. It is important to note that the maximum strengths of the two electric fields are chosen subcritical such that each field by itself is not able to produce pairs. While we choose the maximum value of E to be larger than E_c, the width of each field is so narrow that an electron would be accelerated to a kinetic energy much less than $2c^2$. Note that the Schwinger criterion applies only to an infinitely extended field. We also choose $D \gg W$ such that the spatial overlap of the two electric fields is negligible. The figure also displays the corresponding double Sauter [31] electric potential, defined as $V(z) = -\int_{-\infty}^{z} dz'\, \mathsf{E}(z') = V_1[1 + \tanh(z/W]/2 + V_2\{1 + \tanh[(z - D)/W]\}/2$, where V_1 and V_2 are the heights of two subcritical potentials with amplitudes $V_1 = \mathsf{E}_1 W$ and $V_2 = \mathsf{E}_2 W$.

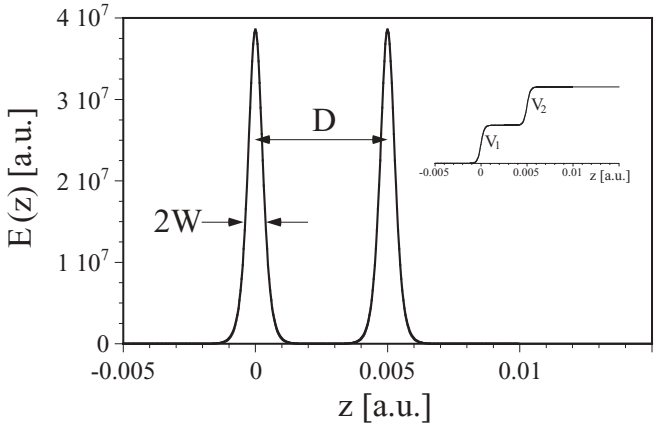

FIG. 1. The two electric fields $\mathsf{E}(z) = (\mathsf{E}_1/2)\text{sech}^2(z/W) + (\mathsf{E}_2/2)\text{sech}^2[(z - D)/W]$ and their associated potential $V(z) = -\int_{-\infty}^{z} dz'\, E(z')$. We have graphed the field and the potential for the parameters used in the simulations discussed below, $D = 0.005$ a.u. and $W = 0.05/\text{c}$].

For simplicity we have turned the potential on instantly at time $t = 0$. In Fig. 2 we show how the number of created electron-positron pairs changes as a function of time for four different interforce separations D ranging from $D = 0$ to $D = 0.03$ a.u.

We note that each graph is characterized by three different temporal regimes. At very early times, directly after the sudden onset of the two fields, the number of pairs grows first quadratically in time $N(t) \sim t^2$. This is generally associated with the abrupt turn-on of the fields. A comparison of the graphs suggests that this early time growth behavior is rather independent of D. In other words, this initial growth can be viewed as the result of an incoherent process due to each (subcritical) electric field pulse, where the created particles at one force location do not have sufficient time to affect the creation process (via Pauli blocking [27,28,32]) at the other location.

The next time regime depends strongly on the spatial shape of the fields. In each case, the long-time behavior is characterized by a permanent linear growth in time, $N(t) \sim St$, where the corresponding pair-creation rate $S = S(V_1, V_2, D)$ depends crucially on the interfield separation D. In other words, the graphs show that even though each of the electric fields is subcritical and time independent, this field configuration is able to produce a permanent flow of electron-positron pairs.

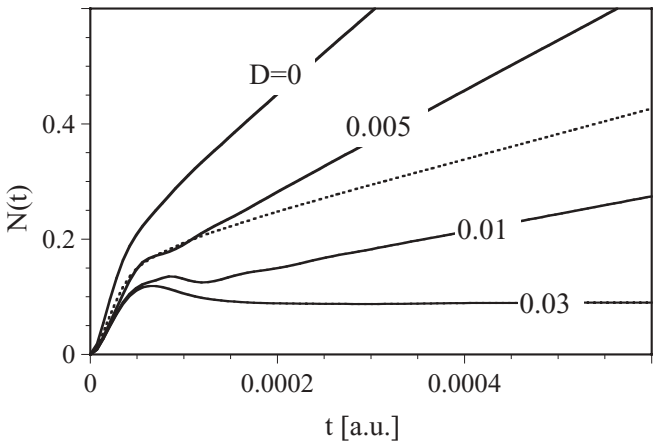

FIG. 2. The electron-positron pair-creation probability $N(t)$ due to the two subcritical fields shown in Fig. 1. The number beside each graph denotes the D chosen in the simulations with $V_1 = V_2 = 1.5c^2$ and $W = 0.05/c$. The dashed line was obtained from a single supercritical field with potential height $V = 2.5c^2$. (Numerical simulation parameters: Length of the numerical box $L = 0.15$ a.u., number of spatial grid points $N_z = 512$, and temporal grid points $N_t = 1000$).

In order to better estimate the magnitude of this effect, for comparison we have also included in the figure (dashed line) the number of created pairs for a single supercritical electric field with strength $V = 2.5c^2$. The slope of this graph is similar to the one obtained by two pulses with strength $V_1 = V_2 = 1.5c^2$ and separation $D = 0.01$ a.u. and far less than the slope for $D = 0.005$ a.u. This comparison nicely illustrates that even though each electric field has only 60% of the amplitude of the supercritical single pulse, the resulting pair creation can be much stronger. In fact, for $D \to 0$ we approach the production rate of a single electric field with supercritical amplitude $V_1 + V_2 = 3c^2$.

Once the distance D is too large ($D > 0.03$ a.u.), the slope of $N(t)$ approaches zero and there is almost no permanent particle growth. Any particle pair is then created exclusively during the temporal phase when the fields are turned on. It is obvious that using multiple field configurations, the creation dynamics of particles can be controlled.

III. THE PAIR-CREATION RATE AND ITS RELATIONSHIP TO THE TRANSMISSION COEFFICIENT

In this section we will focus on the relationship of the long-time pair-creation rate S with the transmission coefficient associated with a (physically different) situation where a single incoming electron scatters off of the same field configuration that produces the electron-positron pairs. Based on an original conjecture by Hund [33], one can show that the rate can be obtained from the energy integral over the transmission coefficient [16,34], as

$$S = \frac{1}{2\pi} \int_{c^2}^{V-c^2} T(E) dE. \tag{2}$$

This surprisingly simple relationship follows from the underlying structure of the energy eigenstates associated with the Dirac Hamiltonian given in Eq. (1). It is valid for the energy regime $c^2 < E < V - c^2$ with $V > 2c^2$, at which a portion of the wave function (modeling an incoming particle) can actually penetrate the potential barrier of total height V. This purely mathematical transmission, however, does not mean that an actual physical electron can pass through this barrier as its energy E is less than the barrier height V. This mathematical property of the Dirac (and also of the Klein-Gordon) equations is related to the famous Klein paradox [25–28].

As this transmission is quite useful to understand the quantum field theoretical pair-creation process, we illustrate here the dynamics of the underlying quantum-mechanical system. In such a simulation, we approximate the initial state of the incoming electron by a Gaussian wave packet with the two-component wave function:

$$\phi(z, t = 0) \equiv N_m \begin{pmatrix} 1 \\ \frac{p}{c+\sqrt{c^2+p^2}} \end{pmatrix} \exp[ipz - (z - z_0)^2/(2\Delta z)^2]. \tag{3}$$

Here N_m denotes the normalization factor such that the total norm is equal to 1, which is conserved in time as H is unitary. The spatial width is denoted by Δz and p is the central momentum corresponding to the incoming energy. The spatial length of the numerical box is 30 a.u. The wave packet is initially localized at $z_0 = -6$ a.u.

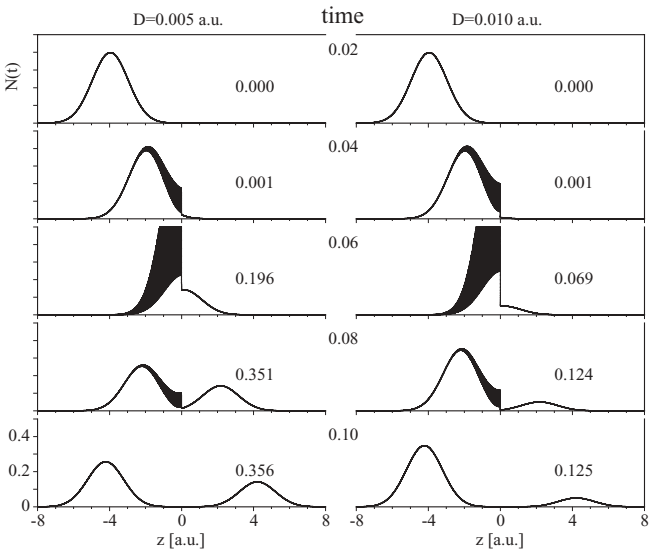

FIG. 3. Snapshots of the charge density for the quantum-mechanical scattering off the two-field configuration shown in Fig. 1 with a spacing $D = 0.005$ a.u. (left) and $D = 0.01$ a.u. (right), taken at times separated by the interval $\Delta t = 0.02$ a.u. The incoming energy $E = 1.5c^2$ corresponds to a central momentum of $p = (5/4)^{1/2}c$. The numbers next to the densities are the corresponding total probabilities for $z > D$. (Numerical parameters: Length of the numerical box $L = 30$ a.u., number of spatial grid points $N_z = 65{,}536$, and temporal grid points $N_t = 20{,}000$, $W = 0.05/c$].

In Fig. 3 we describe the time evolution of the charge density approaching the two fields that are located at $z = 0$ and $z = D$. The computational algorithm is similar to the split-operator method described in the appendix. The electron wave packet enters the potential region from the left side, interacts with the two electric force fields, and splits into the reflected and transmitted parts. The interaction with the field is characterized by the occurrence of high-frequency oscillations based on the interference of incoming and reflected portions of ϕ, whose wavelength is related to the incoming momentum p. We compare the time evolution for two different field configurations; the left sequence is for the interforce separation $D = 0.005$ a.u., while the snapshots in the right column are for $D = 0.01$ a.u.

In order to test the validity of Eq. (2), we compute the total area of the transmitted portion of the charge density to determine the transmission coefficient for that particular incoming energy E. The final transmission coefficients for the Gaussian wave packet amount to $T = 0.356$ for $D = 0.005$ a.u. and $T = 0.125$ for $D = 0.01$ a.u., respectively. We will see in Sec. IV that the amount of the transmitted wave packet portion and the transmission coefficient decrease exponentially with increasing field separation D, suggesting that tunneling is the main mechanism leading to this effect. A more global description of the relationship between these key parameters will be presented in the next section based on a stationary state analysis that will permit us to compare our numerical data with analytical results.

IV. THE TRANSMISSION COEFFICIENT FOR NARROW FIELDS

In this section we will derive an analytical expression for the transmission coefficient $T(E,V_1,V_2,D)$ and use its energy integral to predict the long-time pair-creation rate $S(V_1,V_2,D)$ according to Eq. (2). This will permit us to compare the rates with the long-time slopes $dN(t)/dt$ obtained from the quantum field theoretical number of created pairs.

Here we will focus on the narrow-field limit $W \to 0$, for which the potential becomes $V(z) \to V_1\theta(z) + V_2\theta(z-D)$, where $\theta(\ldots)$ denotes the Heaviside unit-step function, defined as $\theta(z) \equiv (1 + |z|/z)/2$. This choice has two advantages; first, for any distance $D \neq 0$, the two electric fields have a completely vanishing spatial overlap that will permit an unambiguous interpretation of the results in terms of tunneling. Secondly, this special case leads to analytical expressions for the pair-production rate that can be compared with the long-time limit of the time-dependent particle numbers.

In order to determine the transmission coefficient, we have to find the stationary energy eigenstates for the Hamiltonian $c\alpha_z + \beta c^2 + V(z)$ with the two narrow fields located again at $z = 0$ and D. As a result there are three spatial regions for which the electric field vanishes, region I ($z < 0$), region II between both electric fields ($0 < z < D$), and region III to the right of both fields ($D < z$).

In region I the potential height is zero, such that the momentum of the incoming and reflected state is $p \equiv (1/c)\sqrt{(E^2 - c^4)}$. In region II the subcritical potential height is less than the incoming energy $E < V_1$; the wave function decays or grows exponentially with a factor $\beta \equiv (1/c)\sqrt{[c^4 - (V_1 - E)^2]}$ characteristic of quantum-mechanical tunneling. In region III, the potential provides nondecaying states with the momentum $q \equiv (1/c)\sqrt{[(V_1 + V_2 - E)^2 - c^4]}$. The relevant wave functions can be written as

$$\Phi_{\rm I} = \frac{1}{\sqrt{2\pi}}\frac{1}{\sqrt{2E}}\begin{pmatrix}\sqrt{E+c^2}\\ \sqrt{E-c^2}\end{pmatrix}e^{ipz} + \frac{1}{\sqrt{2\pi}}\frac{r}{\sqrt{2E}}\begin{pmatrix}\sqrt{E+c^2}\\ -\sqrt{E-c^2}\end{pmatrix}e^{-ipz}, \tag{4a}$$

$$\Phi_{\rm II} = A\frac{1}{\sqrt{2\pi}}\begin{pmatrix}\sqrt{c^2-(V_1-E)}\\ -i\sqrt{c^2+(V_1-E)}\end{pmatrix}e^{\beta z} + B\begin{pmatrix}\sqrt{c^2-(V_1-E)}\\ i\sqrt{c^2+(V_1-E)}\end{pmatrix}e^{-\beta z}, \tag{4b}$$

$$\Phi_{\rm III} = \frac{1}{\sqrt{2\pi}}\frac{t}{\sqrt{2(V_1+V_2-E)}} \times \begin{bmatrix}\sqrt{(V_1+V_2-E)-c^2}\\ \sqrt{(V_1+V_2-E)+c^2}\end{bmatrix}e^{-iqz}|J|. \tag{4c}$$

The parameters r and t are the reflection and transmission amplitudes and we have $T = |t|^2|J|$. By matching wave functions at the boundaries $z = 0$ and D, we can find the expansion amplitudes A and B and after some cumbersome calculations derive the transmission coefficient T as

$$T(E,V_1,V_2,D) = \frac{2c^2pq}{2c^2V_1V_2\sinh^2(\beta D)/\beta^2 + E(V_1+V_2-E) + c^2pq + c^4}. \tag{5}$$

Note that the expression depends asymmetrically on V_1 and V_2. However, when integrated over the energy E the result is symmetric about the sequence of V_1 and V_2 as one might have expected. For large spacing D, the transmission coefficient falls off exponentially with increasing D, $T = 4\beta^2pq/(V_1V_2)exp(-2\beta D)$, as characteristic of a tunneling effect. In the opposite limit, $D = 0$, T is characteristic of a single barrier with height $V_1 + V_2$.

In order to test the validity of this formula, we compare its prediction with the actual transmission coefficients obtained from the area of the transmitted wave function portion obtained in the quantum-mechanical wave packet simulation of the previous section.

In Fig. 4 we compare the analytical expression for T from Eq. (5) with the numerical transmission data (circles) for the small width $W = 0.05/c$ as a function of the separation D for two incoming energies $E = 1.2c^2$, and $1.5c^2$. The agreement is superb. The two black dots represent the transmission coefficients $T = 0.125$ and 0.356, for which the time evolution was presented in Fig. 3. The small amount of discrepancy is expected and associated with the finite width of the wave packet used in the simulations leading to Fig. 3.

As a next step we compute the actual pair-creation rates S via the energy integral over the analytical transmission coefficient according to Eq. (2). As the energy E is contained in the momenta p and q, and in the tunneling length β^{-1}, this integral must be determined numerically in general.

In Fig. 5 we compare the analytical rate with the actual slope of the time-dependent number of particle pairs $N(t)$ obtained from quantum field theory. We can see that the results

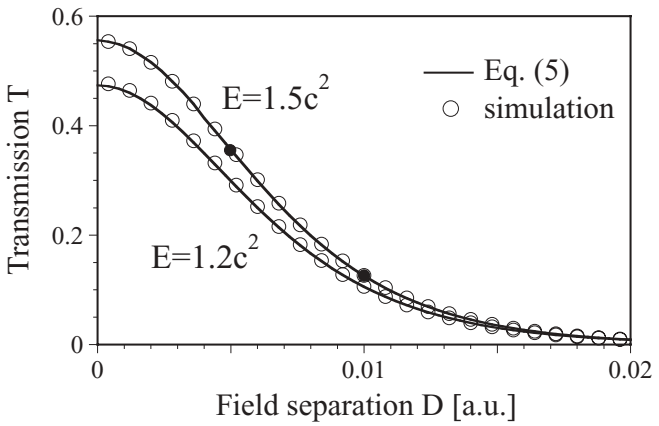

FIG. 4. The transmission coefficient T as a function of the distance D for electrons with two different incoming energies, $E = 1.5c^2$ and $1.2c^2$. Solid lines are predicted by Eq. (5). The circles are the corresponding transmission coefficient obtained from the time-dependent wave packet simulations while the two solid circles indicate the transmission coefficient from Fig. 3.

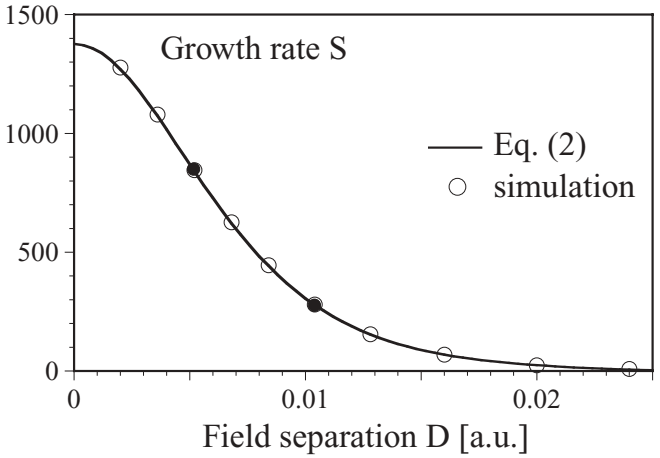

FIG. 5. The pair-creation growth rate S as a function of the distance D of the two electric fields. Solid lines are the predictions by Eqs. (2) and (5) for $W \to 0$. The circles are the corresponding growth rates obtained from the time-dependent simulations while the solid circles indicate the slopes in Fig. 2. (Numerical simulation parameters: Length of the numerical box $L = 0.15$ a.u., number of spatial grid points $N_z = 512$, and temporal grid points $N_t = 1000$, $W = 0.05/\mathrm{c}$).

simulated by quantum field theory also match very well with the analytical solution of Eq. (5). The error with the data shown is $<0.1\%$.

V. SUMMARY AND DISCUSSION

In this work, we discussed a theoretical formalism that allows us to compute the time-dependent pair-creation probability for multiple force field configurations under the description of both quantum field theory and quantum mechanics. These studies suggest that there is a third mechanism that can lead to the creation of electron-positron pairs from the vacuum, even if the external electric field is neither supercritical nor rapidly oscillating in time. The formal mathematical relationship between the asymptotic pair-creation rate and the transmission coefficient permits us to study complicated field configurations relatively easily. Instead of carrying out involved quantum field theoretical computations, one can optimize the transmission for a special field arrangement. Based on this relationship one can loosely associate this third mechanism with quantum tunneling.

In order to avoid potential confusion, we should mention that in the case of a supercriticality induced pair creation, the corresponding quantum scattering system is characterized by a nonvanishing transmission coefficient, based on the fact that there are energetically permitted nondecaying (nontunneling) states under the potential step barrier leading to a nonvanishing transmission. This particular mechanism has sometimes been called "Klein tunneling" [26], even though in contrast to our mechanism, there are no exponentially decaying states involved.

The effect of tunneling on the pair-creation mechanism also contributes to the general discussion about whether global properties such as the potential and its resulting energy levels or local properties such as the electric field strength at certain spatial regions are more important for the pair-creation process. Traditionally, the diving of the lowest-lying bound state into the negative energy continuum has been associated with the onset of pair creation [1]; on the other hand, spatially resolved simulations show that the particles are being created only at those local regions where the force field is maximum [32]. To examine this question further, we simulated the pair-creation process for a potential well with an increase of the width of the well while leaving the regions of largest force (the wings of the well) unchanged. We observed a clear onset of supercriticality at widths where the lowest-energy eigenstate shifts into the negative energy continuum. The results suggest that the location of lowest-energy eigenstate plays a crucial part during pair creation. These studies are also slightly more complicated as one has to rely entirely on quantum field theoretical simulations because the analogous quantum scattering system does not permit Klein tunneling and the long-time creation rate vanishes due to Pauli blocking [32].

The observation also raises interesting questions about the locality and causality of the pair-creation process under external fields [35]. As the two electric fields did not overlap, the early charge densities associated with the created particles at each location also should not overlap, suggesting that at early times, the turn-on induced initial growth of particles growth at each location are completely independent of each other. Only once the particles created at one location have propagated to the other region, does the system evolve into its steady state pair-creation mode.

A possible experimental set-up would be obviously much more complicated than described by our oversimplified model system. But in view of the difficulty to generate supercritical fields, we point out that having a sequence of multiple external fields (even if they do not or only minimally overlap) could help to enhance the chance of detecting electron-positron pairs in this experimentally challenging endeavor.

ACKNOWLEDGMENTS

We enjoyed several helpful discussions with R. Wagner. This work has been supported in part by the NSFC (Grants No. 10734130 and No. 10925421), the National Basic Research Program of China (Grant No. 2007CB815105), and by the NSF. Q. S. acknowledges the hospitality by the CAS where this work was initiated. We also acknowledge support from the Research Corporation.

APPENDIX

In computational quantum field theory, $\hat{\Psi}(t)$ is the field operator for the electron-positron complex. As a hybrid of an operator and a quantum-mechanical wave function it satisfies not only the Heisenberg equation of motion but also the ordinary Dirac equation given by Eq. (1). We can expand $\hat{\Psi}(t)$ into terms of creation and annihilation operators in the energy range $c^2 < E < V - c^2$, where the particle is expected to be created and ignore other terms outside this range.

$$\hat{\Psi}\ (t) = \sum_p \hat{b}_p(t)\,|p\rangle + \sum_n \hat{d}_n^{\dagger}(t)\,|n\rangle. \qquad \text{(A1)}$$

Here the states $|p\rangle$ and $|n\rangle$ denote the quantum-mechanical energy eigenstates of the force-free Hamiltonian and the subscripts p and n represent positive and negative energy, respectively. These eigenstates are time evolved under the whole Hamiltonian with the external field interaction leading to $|p(t)\rangle$ and $|n(t)\rangle$. The creation and annihilation operators satisfy the fermionic anticommutator relationship $[\hat{b}_p, \hat{b}^\dagger_{p'}]_+ = \delta(p-p')$ and $[\hat{d}_n, \hat{d}^\dagger_{n'}]_- = \delta(n-n\prime)$. These operators evolve in time according to

$$\hat{b}_p(t) = \sum_{p'} \hat{b}_{p'}\langle p|p'(t)\rangle + \sum_n \hat{d}^\dagger_n \langle p|n(t)\rangle = \sum_{p'} \hat{b}_{p'} U_{p,p'}(t) + \sum_n \hat{d}^\dagger_n U_{p,n}(t), \tag{A2a}$$

$$\hat{d}^\dagger_n(t) = \sum_p \hat{b}_p\langle n|p(t)\rangle + \sum_{n'} \hat{d}^\dagger_{n'}\langle n|n\prime(t)\rangle = \sum_p \hat{b}_p U_{n,p}(t) + \sum_{n'} \hat{d}^\dagger_{n'} U_{n,n'}(t). \tag{A2b}$$

The matrix elements $U_{p,p'} = \langle p|p'(t)\rangle$, $U_{p,n} = \langle p|n(t)\rangle$, $U_{n,p} = \langle n|p(t)\rangle$, and $U_{n,n'} = \langle n|n'(t)\rangle$ can be computed from the evolution of the single-particle Dirac equation. The solution of Eq. (1) can be used to calculate various quantum field theoretical observables. For the pair-creation process we need to compute the corresponding expectation value in the fermionic vacuum state $||\text{vac}\rangle\rangle$. To analyze the total pair creation, first we compute the average particle density $\rho^{(p)}(z,t)$ of the created electrons by using the density operator $\hat{\Psi}^{\dagger(p)}(z,t)\hat{\Psi}^{(p)}(z,t)$.

For electrons, which have positive energies, the space-time-dependent field operator is

$$\hat{\Psi}^{(p)}(z,t) = \sum_p \hat{b}_p(t) w_p(z), \tag{A3}$$

where $w_p(z)$ denotes the two-component spatial representation of the eigenvector of force-free Hamiltonians with positive energy. With Eq. (A3) and Eq. (A2a), the probability density of the electrons is

$$\rho(z,t) = \langle\langle \text{vac}||\hat{\Psi}^{\dagger(p)}(z,t)\hat{\Psi}^{(p)}(z,t)||\text{vac}\rangle\rangle = \sum_n \left|\sum_p U_{p,n}(t) w_p(z)\right|^2 \tag{A4}$$

By integrating the probability density spatially, we obtain the average number of created electrons as

$$N(t) = \sum_{pn} |U_{p,n}(t)|^2. \tag{A5}$$

In order to compute $U_{p,n} = \langle p|n(t)\rangle$, we solve the single-particle Dirac equation starting from negative energy state $|n\rangle$ at $t = 0$. The single-particle Dirac equation is solved numerically by the split-operator technique [18–21]. In this method the time-evolution operator $\exp[-iht]$ is decomposed into N_t consecutive actions; each subinterval operators can be approximated by $\exp(-iht) \approx \exp[(-iV\Delta t/2)(-ih_0\Delta t)(-iV\Delta t/2)]$, where h_0 denotes the force-free Hamiltonian. The action of $\exp(-iV\Delta t/2)$ can be performed conveniently in the discretized coordinate space with N_z grid points. By using the Fourier transformation between spatial and momentum spaces, we can compute the action of the corresponding propagators via simple multiplications in the relevant space.

[1] W. Greiner, B. Müller, and J. Rafelski, *Quantum Electrodynamics of Strong Fields* (Springer, Berlin, 1985).
[2] J. Schwinger, Phys. Rev. **82**, 664 (1951).
[3] E. Brezin and C. Itzykson, Phys. Rev. D **2**, 1191 (1970).
[4] V. S. Popov, JETP Lett. **13**, 185 (1971).
[5] D. B. Blaschke, A. V. Prozorkevich, C. D. Roberts, S. M. Schmidt, and S. A. Smolyansky, Phys. Rev. Lett. **96**, 140402 (2006).
[6] A. R. Bell and J. G. Kirk, Phys. Rev. Lett. **101**, 200403 (2008).
[7] G. R. Mocken, M. Ruf, C. Müller and C. H. Keitel, Phys. Rev. A **81**, 022122 (2010).
[8] D. L. Burke *et al.*, Phys. Rev. Lett. **79**, 1626 (1997).
[9] H. Hu, C. Müller and C. H. Keitel, Phys. Rev. Lett. **105**, 080401 (2010).
[10] H. R. Reiss, Eur. Phys. J. D **55**, 365 (2009).
[11] T. Cowan *et al.*, Phys. Rev. Lett. **56**, 444 (1986).
[12] I. Ahmad *et al.* (APEX Collaboration), Phys. Rev. Lett. **78**, 618 (1997).
[13] For a proposal for the development of the ELI project, see [http://www.extreme-light-infrastructure.eu].
[14] R. Schützhold, H. Gies, and G. Dunne, Phys. Rev. Lett. **101**, 130404 (2008).
[15] M. Ruf, G. R. Mocken, C. Müller, K. Z. Hatsagortsyan, and C. H. Keitel, Phys. Rev. Lett. **102**, 080402 (2009).
[16] T. Cheng, Q. Su, and R. Grobe, Phys. Rev. A **80**, 013410 (2009).
[17] S. S. Bulanov, V. D. Mur, N. B. Narozhny, J. Nees, and V. S. Popov, Phys. Rev. Lett. **104**, 220404 (2010).
[18] A. D. Bandrauk and H. Shen, J. Phys. A **27**, 7147 (1994).
[19] J. W. Braun, Q. Su, and R. Grobe, Phys. Rev. A **59**, 604 (1999).
[20] G. R. Mocken and C. H. Keitel, Comput. Phys. Commun. **178**, 868 (2008).
[21] M. Ruf, H. Bauke, and C. H. Keitel, J. Comput. Phys. **228**, 9092 (2009).
[22] T. Cheng, Q. Su, and R. Grobe, Contemp. Phys. **51**, 315 (2010).
[23] P. Krekora, Q. Su, and R. Grobe, Phys. Rev. Lett. **93**, 043004 (2004).
[24] T. D. Newton and E. P. Wigner, Rev. Mod. Phys. **21**, 400 (1949).
[25] B. R. Holstein, Am. J. Phys. **66**, 507 (1998).

[26] N. Dombey and A. Calogeracos, Phys. Rep. **315**, 41 (1999).
[27] P. Krekora, Q. Su, and R. Grobe, Phys. Rev. Lett. **92**, 040406 (2004).
[28] R. E. Wagner, M. R. Ware, Q. Su, and R. Grobe, Phys. Rev. A **81**, 024101 (2010).
[29] P. Krekora, Q. Su, and R. Grobe, Phys. Rev. A **73**, 022114 (2006).
[30] C. C. Gerry, Q. Su, and R. Grobe, Phys. Rev. A **74**, 044103 (2006).
[31] F. Sauter, Z. Phys. **69**, 742 (1931); **73**, 547 (1931).
[32] P. Krekora, K. Cooley, Q. Su, and R. Grobe, Phys. Rev. Lett. **95**, 070403 (2005).
[33] F. Hund, Z. Phys. **117**, 1 (1940).
[34] T. Cheng, M. R. Ware, Q. Su, and R. Grobe, Phys. Rev. A **80**, 062105 (2009).
[35] T. Cheng, S. P. Bowen, C. C. Gerry, Q. Su, and R. Grobe, Phys. Rev. A **77**, 032106 (2008).